

Modifications to the Cauchy–Born rule: Applications in the deformation of single-walled carbon nanotubes

Karthick Chandraseker^a, Subrata Mukherjee^{a,*}, Yu Xie Mukherjee^b

^a *Department of Theoretical and Applied Mechanics, Kimball Hall, Cornell University, Ithaca, NY 14853, United States*

^b *39 Hickory Circle, Ithaca, NY 14850, United States*

Received 7 December 2005; received in revised form 4 March 2006

Available online 20 March 2006

Abstract

This paper presents a study of the Cauchy–Born (CB) rule as applied to the deformation analysis of single-walled carbon nanotubes (SWNTs) that are modeled as 2-dimensional manifolds. The C–C bond vectors in the SWNT are assumed to deform according to the local deformation gradient as per the CB rule or a modified version thereof. Aspects of the CB rule related to spatial inhomogeneity of the deformation gradient at the atomic scale are investigated in the context of a specific class of extension–twist deformation problems. Analytic expressions are derived for the deformed bond lengths using the standard CB rule as well as modified versions of the standard CB rule. Since the deformation map is conveniently *prescribed* in this work, it is possible to compare the performance of these deformation rules with the exact solution (i.e. the exact analytic expression for the deformed bond vectors) given directly by the deformation map. This approach provides insights into the CB rule and its possible modifications for use in more complicated deformations where an explicit deformation map is not available. Specifically, it is concluded that in the case of inhomogeneous deformations at the atomic scale for which the CB rule is only approximate (as demonstrated in Section 1 of this paper), the mean value theorem in calculus can be used as a guide to modify the CB rule and construct a more rigorous and accurate atomistic–continuum connection. The deformed bond lengths are used to formulate an enriched continuum hyperelastic strain energy density function based on interatomic potentials (the multi-body Tersoff–Brenner [Tersoff, J., 1988. New empirical approach for the structure and energy of covalent systems. *Phys. Rev. B* 37, 6991–7000; Brenner, D.W., 1990. Empirical potential for hydrocarbons for use in simulating the chemical vapor deposition of diamond films. *Phys. Rev. B* 42, 9458–9471] empirical interatomic potential for carbon–carbon bonds is used in this work). The deformation map (and hence the deformation gradient, the bond vectors and the continuum strain energy density) contains certain parameters, some of which are imposed and others determined as a result of energy minimization in the standard variational formulation. Numerical results for kinematic coupling and binding energy per atom are presented in the case of imposed extension and twist deformations on representative chiral, zig-zag and armchair nanotubes using the CB rule and its modifications. These results are compared with the exact solution based on the deformation map which serves as a basis for evaluating the efficacy of these deformation rules. The ideas presented in this paper can also be directly extended to other lattices.

© 2006 Elsevier Ltd. All rights reserved.

* Corresponding author. Tel.: +1 607 255 7143; fax: +1 607 255 2011.

E-mail address: sm85@cornell.edu (S. Mukherjee).

Keywords: Atomistic model; Cauchy–Born rule; Constitutive; Continuum; Finite deformation; Homogeneous; Kinematic; Membrane; Nonlinear elasticity; Non-uniform; Variational method

1. Introduction: The Cauchy–Born rule

The Cauchy–Born (CB) rule (Cousins, 1978; Ericksen, 1984) has proven to be effective at linking the deformation of an atomic system to that of a continuum without other phenomenological input. It states that the vector defined by a pair of atoms deforms according to the local deformation gradient, i.e.

$$\mathbf{a} = \mathbf{F}(\mathbf{X}) \cdot \mathbf{A} \tag{1}$$

where \mathbf{A} refers to the undeformed bond vector, \mathbf{a} refers to the deformed bond vector and \mathbf{F} refers to the local deformation gradient at material point \mathbf{X} . This hypothesis describes crystal behavior well as long as the continuum deformation is nearly homogeneous in the scale of the crystal. The CB rule (with a homogeneous \mathbf{F} at the atomic scale) has been successfully applied to space-filling crystals represented as complex Bravais lattices by Tadmor et al. (1999).

The following illustrates the relation between the CB rule and the exact expression for the deformed bond vectors in the case of an arbitrary deformation imposed on a bulk solid (atoms assumed to lie in a 3-dimensional continuum. See Chandraseker and Mukherjee, 2006). By referring to Fig. 1 and from the map $p = \mathcal{F}(P)$, it is seen that:

$$\mathbf{a} = \mathcal{F}(\mathbf{X} + \mathbf{A}) - \mathcal{F}(\mathbf{X}) \tag{2}$$

By expanding the right hand side of (2) in a Taylor series about \mathbf{X} , and using $\mathbf{F} = \nabla \mathcal{F}$, one has

$$\mathbf{a} = \mathbf{F}(\mathbf{X}) \cdot \mathbf{A} + \frac{1}{2!} \nabla \mathbf{F}(\mathbf{X}) : (\mathbf{A} \otimes \mathbf{A}) + \frac{1}{3!} \nabla \nabla \mathbf{F}(\mathbf{X}) \diamond (\mathbf{A} \otimes \mathbf{A} \otimes \mathbf{A}) + \text{h.o.t.} \tag{3}$$

where ‘ \diamond ’ denotes the action of a fourth rank tensor on a third rank tensor that results in a vector, ‘ $:$ ’ denotes the action of a third rank tensor on a second rank tensor that results in a vector, and ‘ \otimes ’ denotes the standard tensor product (see, for example Steigmann and Ogden, 1999). Eq. (3) gives the exact expression for the deformed bond vector (as obtained directly from the deformation map) and shows that the deformed bond vector depends not only on the deformation gradient \mathbf{F} , but on its gradients as well. *If the deformation gradient is constant in space, all its gradients vanish, and the Taylor series reduces to the standard CB rule, which becomes exact in this case.* Hence, the Taylor series holds the key to the degree of homogenization enforced on \mathbf{F} . A key idea to note is that even in the case of inhomogeneous deformations at the atomic scale, if the deformation map \mathcal{F} is differentiable on the closed interval $[\mathbf{X}, \mathbf{X} + \mathbf{A}]$, the mean value theorem in calculus (see, for example

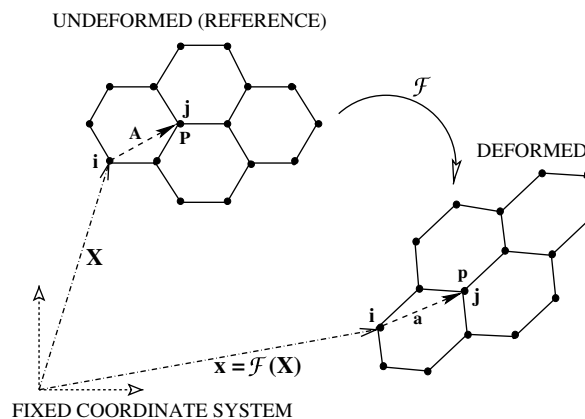


Fig. 1. The direct map $\mathcal{F}(\mathcal{F}(P) = p)$.

Gradshteyn and Ryzhik, 2000) guarantees the existence of some $\mathbf{X}_z \in [\mathbf{X}, \mathbf{X} + \mathbf{A}]$ that allows us to rewrite Eq. (2) in the form:

$$\mathbf{a} = \mathbf{F}(\mathbf{X}_z) \cdot \mathbf{A} \quad (4)$$

This idea provides the intuition for modifying the CB rule to account for inhomogeneous deformations at the atomic scale, as will be subsequently discussed in detail in Section 4. Further, the standard CB rule requires modification if one is interested in problems on 2-D manifolds i.e. that are membrane like. In such cases, (1) needs to be interpreted in terms of \mathbf{F} mapping tangent vectors to the manifold at point \mathbf{X} , from the undeformed to the deformed domains (see, for example Marsden and Hughes, 1983). Here, one can either use a fully 3-dimensional \mathbf{F} or a 2-dimensional *surface* deformation gradient – the actions of both these objects on tangent vectors to 2-dimensional manifolds are identical (see, for example Steigmann and Ogden, 1999).

The present work focuses on a class of deformations that is, in general, assumed to be spatially inhomogeneous at the atomic scale. Specifically, it is concluded that in the case of inhomogeneous deformations at the atomic scale for which the CB rule is only approximate (as demonstrated in Section 1 of this paper), the mean value theorem in calculus can be used as a guide to modify the CB rule and construct a more rigorous and accurate atomistic–continuum connection. This is one of the key contributions of the present paper.

Also, the domain of interest is a single-walled carbon nanotube (SWNT) which is modeled as a thin-walled cylinder – a 2-D manifold. We perform this deformation analysis by adopting the CB rule and suggest possible modifications to account for the spatial inhomogeneity of \mathbf{F} at the atomic scale and the fact that our domain is a 2-D manifold. To deal with inhomogeneities such as defects and non-local effects, mixed continuum–atomistic approaches have been proposed by Tadmor et al. (1996) and Shenoy et al. (1999) in the context of finite element formulations.

In the present work, we employ a 3-dimensional cylindrical deformation gradient evaluated at the surface of the SWNT. Since all the carbon atoms are assumed to lie on the same cylindrical surface, this means that there is no radial variation of \mathbf{F} . Further, in the case of curved membranes, the bond vectors are, in fact, chords and not tangent vectors (and the chord \approx tangent approximation gets worse as the curvature increases). For such domains, the standard CB rule has been extended using the idea of an exponential map by Arroyo and Belytschko (2002). In this modification, the bond lengths are viewed as intrinsic distances in the 2-dimensional continuum which are essentially geodesics connecting the two atoms on the surface. To be able to apply the CB rule in this case, one would first need to ‘unwrap’ the geodesic onto the tangent plane at \mathbf{X} , then apply \mathbf{F} to this geodesic vector to obtain the deformed geodesic vector lying on the deformed tangent plane, and finally ‘wrap’ the deformed geodesic back onto the deformed surface to obtain the Euclidean bond lengths. The exponential map provides the mathematical means to perform the ‘unwrap’ and ‘wrap’ operations described above.

It is again noted (see above) that if a 3-dimensional \mathbf{F} is used in the CB rule with the SWNT atoms assumed to lie in the 3-dimensional continuum, the standard CB rule (without any modification, i.e. using the bond vectors as chords) gives the exact solution if \mathbf{F} is spatially constant (Chandraseker and Mukherjee, 2006). In such an approach, modifications to the CB rule become necessary only if \mathbf{F} is inhomogeneous at the atomic scale.

The CB rule has also been used to connect the atomistic and continuum descriptions of a SWNT by Zhang et al. (2002), Jiang et al. (2003) and Liu et al. (2004). In all these papers, the SWNT deformation analysis is performed by mapping the deformed SWNT back to a planar sheet, and measuring the energies of the atoms on the SWNT by considering their mapped positions on the cylinder. In the present work dealing with the deformation of SWNTs, we consistently assume that bond lengths are measured as Euclidean distances between atoms on the deformed cylinder, and the energies of atoms are measured in the cylindrical configuration.

The present paper is organized as follows. The constitutive model for nonlinear elastic deformation of atomic lattices is presented first. This is based on a quasicontinuum approach in which the continuum hyperelastic strain energy density is expressed in terms of interatomic potentials in the atomic lattice. Next, a generalized deformation map that models coupled extension and twist of a thin-walled circular cylinder is presented, and an analysis of the equivalence between the strong and weak forms of static equilibrium for this proposed deformation map follows. The deformation gradient (\mathbf{F}) derived from this map happens to

be inhomogeneous, in general. Hence, in the context of this coupled extension–twist deformation, we present possible modifications to the CB rule to deal with the inhomogeneity in \mathbf{F} using analytic expressions for the deformed bond lengths derived from different approaches. Finally, we present numerical results to illustrate the suggested modifications in the context of two different deformation problems. In the first problem, we study the coupling between extension and twist deformations imposed on SWNTs, and in the second, we study the variation of the binding energy/atom with imposed extension on SWNTs. A discussion of the results, and some concluding remarks, complete the paper.

2. Constitutive model for nonlinear deformation of single-walled carbon nanotubes

The present section describes the formulation of a continuum hyperelastic strain energy density function based on interatomic potentials. This effectively connects the atomic system to the deformation of the continuum thereby leading to a multi-length scale framework. The essential ideas can also be found in other works dealing with the quasicontinuum method for bulk materials (Tadmor et al., 1996; Shenoy et al., 1999; Tadmor et al., 1999).

2.1. Interatomic potential for carbon

In the present work, a particular atomistic model due to Brenner (1990) is considered. It is assumed that the topology of the bond network does not change, i.e., there is no bond breaking or formation. Following Brenner (1990) and Tersoff (1988), an expression for the bonding energy between atoms i and j for carbon is

$$V(a(i, j)) = V_R(a(i, j)) - \bar{B}(i, j)V_A(a(i, j)) \quad (5)$$

where $a(i, j)$ is the bond length (i.e. the distance between carbon atoms i and j at the two ends of the bond), V_R and V_A are the repulsive and attractive pair terms. The parameter $\bar{B}(i, j)$ in (5) represents a multi-body coupling between the bond from atom i to atom j , and the local environment of atom i . The potential given by Brenner (1990) contains two sets of parameters. The first set is a good fit (with experiments) for the bond lengths, while the second fits the stretching force constants well. The cylindrical positions of the atoms are generated by mapping a planar graphene sheet to a cylindrical SWNT based on its chirality. This models the rolling process of a planar sheet of graphene into a cylindrical SWNT. The energy of a representative atom on the cylindrical SWNT is minimized with respect to certain lengths in the planar graphene sheet. The details on this stage of calculations can be found in Chandraseker and Mukherjee (2006). During this process, we make natural symmetry-based assumptions on the bond lengths and angles of the next-to-nearest neighbors of this representative atom. These assumptions are based on the periodicity of the hexagonal graphene lattice and hold good during the deformation simulations as well. These were implemented approximately in the earlier work by Chandraseker and Mukherjee (2006). In the present work, they are implemented exactly as follows.

A representative atom ‘ A ’, and the surrounding atoms that influence its energy (according to the Brenner interatomic potential) are shown for the case of a zig-zag and armchair SWNT (see Fig. 2). The atoms can be considered to be lying on a planar graphene sheet. In the figure, Γ indicates the circumferential direction after roll-up and Λ indicates the axial direction. The roll-up axis depends on the atomic structure of the SWNT (depending on whether the SWNT is armchair, zig-zag or chiral). The bond lengths between atoms on the rolled-up cylinder can be found by using a map (details can be found in Chandraseker and Mukherjee (2006)). The relationships between these bond lengths are summarized in Box 1.

These relationships are used to obtain bond lengths and angles which are required to calculate the energy for the representative atom A (see Fig. 2) as per the Brenner interatomic potential, and hold good during imposed deformation as well, based on assumed periodicity of the atomic lattice.

2.2. Nonlinear elastic deformation of the atomic lattice

The starting point here is the undeformed SWNT with the atom positions obtained as described above. The deformation gradient $\mathbf{F} = \partial\mathbf{x}/\partial\mathbf{X}$, where \mathbf{X} and \mathbf{x} denote the positions of a material point in the undeformed

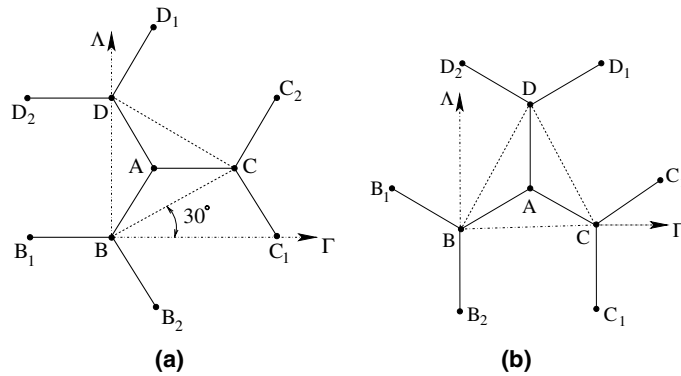


Fig. 2. Atomic structure for (a) armchair, and (b) zig-zag SWNTs. The figures show nearest neighbors B, C, D of atom A , and the nearest neighbors of B, C, D .

$a(B, B_1) = a(C, A)$	$a(D, D_2) = a(C, A)$
$a(B, B_2) = a(D, A)$	$a(C, C_1) = a(D, A)$
$a(C, C_2) = a(B, A)$	$a(D, D_1) = a(B, A)$
$a(A, B_1) = a(C, B)$	$a(A, B_2) = a(D, B)$
$a(A, C_1) = a(D, C)$	$a(A, C_2) = a(B, C)$
$a(A, D_1) = a(B, D)$	$a(A, D_2) = a(C, D)$

Box 1. Relationships between the C–C Euclidean lengths for all SWNTs.

and deformed configurations, respectively. In the following equations, $\mathbf{A}(i, j)$ and $\mathbf{a}(i, j)$ denote the undeformed and deformed bond vectors, respectively, in the case of a bulk crystal. For simplicity, analysis using the standard CB rule (1) (applicable for bulk materials) is presented in this section. For curved membranes, however, we adopt the modified CB rule discussed in Section 1, and view these bond vectors as geodesic vectors projected onto the appropriate (undeformed or deformed) tangent plane. The details of the wrapping/unwrapping operations along with the expressions for the bond vectors are presented in Section 4 of this paper.

Using the CB rule (1), one can obtain:

$$a^2(i, j) = \mathbf{A}(i, j) \cdot (\mathbf{I} + 2\mathbf{E}) \cdot \mathbf{A}(i, j) \quad (6)$$

where the Lagrangian strain $\mathbf{E} = \frac{1}{2}(\mathbf{F}^T \cdot \mathbf{F} - \mathbf{I})$ with \mathbf{I} the second order identity tensor, and \mathbf{F}^T is the transpose of \mathbf{F} . A centrosymmetric (simple Bravais) lattice is one that has pairs of bonds in opposite directions around each atom. The CB rule ensures equilibrium for such a structure for arbitrary imposed homogeneous deformations. A SWNT, however, is not centrosymmetric, but consists of two different sub-lattices (a Bravais multi-lattice), each of which is centrosymmetric. An in-plane shift vector ζ becomes necessary (when using the CB rule) in such a case to relate an atom pair when each of the atoms in the pair lies on different sub-lattices (see, for example Tadmor et al., 1999; Zhang et al., 2002; Jiang et al., 2003; Liu et al., 2004). By defining $\zeta = \mathbf{F} \cdot \boldsymbol{\eta}$, one has a modified version of the CB rule as follows:

$$\mathbf{a}(X, Y) = \mathbf{F} \cdot \mathbf{A}(X, Y) + \zeta = \mathbf{F} \cdot (\mathbf{A}(X, Y) + \boldsymbol{\eta}) \quad (7)$$

(with $\zeta = \mathbf{F} \cdot \boldsymbol{\eta}$) when atoms X and Y belong to different sub-lattices; and $\boldsymbol{\eta} = 0$ otherwise. It is noted from above that a deformed bond length a , in general, is a function of \mathbf{E} and $\boldsymbol{\eta}$. In practice, one can account for the shift vector by providing additional degrees of freedom to the coordinates of the representative central atom in the undeformed configuration, and finding these additional displacements by minimizing energy/atom for each imposed deformation. In the present work, since the continuum is essentially 2-dimensional, $\boldsymbol{\eta}$ has

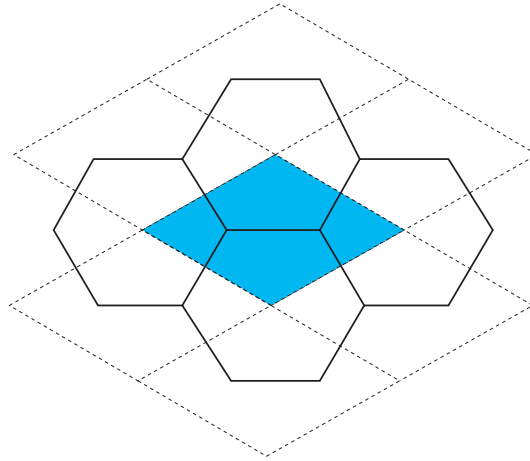


Fig. 3. The shaded parallelogram shown above is the unit cell in a graphene sheet.

only in-plane components (specifically, with respect to a cylindrical basis, the only allowed components are η_{θ} and η_z with the radial component constrained to be zero). Since the internal relaxation due to the shift vectors is applied to the reference configuration, material frame indifference of the deformed bond lengths to rigid body rotations is automatically guaranteed. In fact, this guarantees frame-indifference even when the exact deformed bond lengths are determined by using the direct map (3) later in this paper. This implementation approach also ensures that the presence of the internal relaxation does not affect the analytic expressions for the deformed bond vectors derived subsequently in the paper. In all of the above equations involving \mathbf{F} or \mathbf{E} , it is important to note that when the deformation is inhomogeneous, these tensors need to be evaluated at a specific point on each bond in order to apply the above equations and obtain the deformed bond lengths. This issue will be addressed in a subsequent section.

2.3. Strain energy density expressed in terms of interatomic potentials

The deformed bond lengths obtained from (7) are used along with (5) to define a hyperelastic continuum strain energy density W for this membrane model of a SWNT. We consider a representative unit cell of the lattice indicated in Fig. 3 containing two carbon atoms (Dresselhaus et al., 2004). In view of the two atom basis for graphene, its entire structure can be generated by replicating the parallelogram in Fig. 3. This leads to the following definition of W (see, for example Arroyo and Belytschko, 2002; Zhang et al., 2002):

$$W(\mathbf{E}, \boldsymbol{\eta}(\mathbf{E})) \equiv \hat{W}(\mathbf{E}) = \frac{\sum_{\text{cell}} V(a(i, j))}{\Omega_{\text{cell}}} \quad (8)$$

where the bond energies are summed over the domain of the representative unit cell of area Ω_{cell} in the cylindrical configuration. This area is assumed to be preserved while rolling up a planar graphene sheet, and hence can be computed from the planar configuration shown in Fig. 3. It is important to mention here that the strain energy density function W must satisfy material frame indifference to rigid body rotations. Since W depends only on the deformed bond lengths which have been shown to be frame-indifferent in the previous sub-section, this requirement is automatically satisfied. This hyperelastic strain energy density also depends on the undeformed crystal structure and inherits its symmetries. Further, when the deformation is inhomogeneous, \mathbf{E} varies in space. However, the above definition of W implies that as long as the deformed bond lengths are obtained by evaluating \mathbf{E} at a specific point on each bond, W is *uniform* over the unit cell (i.e. it does not contain an explicit spatial variation within the unit cell). This leads to an approximation of the total energy in the domain as the simple sum of unit cell energies, thereby leading to a multi-length scale enriched continuum framework.

$$\begin{aligned} r &= \gamma R \\ \theta &= \Theta + f(Z; k) \\ z &= (1 + \epsilon)Z \end{aligned}$$

Box 2. The direct deformation map.

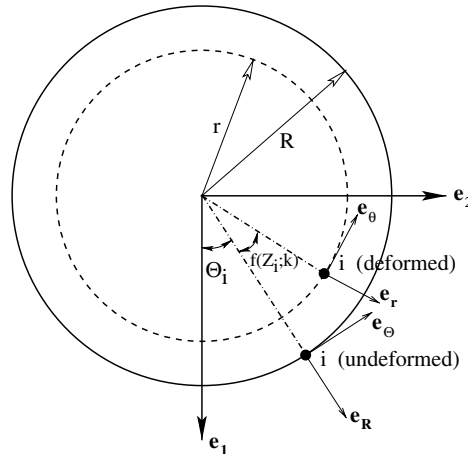


Fig. 4. Undeformed and deformed cross-sections of a SWNT.

3. Generalized extension and twist of a thin-walled circular cylinder

A generalized extension–twist deformation map is chosen for analysis. In terms of standard cylindrical coordinates, this is conveniently displayed in Box 2 (see Fig. 4), where r and R are the deformed and undeformed radii of the cylinder, respectively (the cylinder is assumed to be thin-walled), γ is a constant, θ and Θ are respectively the deformed and undeformed polar angles on the cylindrical cross-section, z and Z are the deformed and undeformed axial coordinates, respectively, ϵ is the axial strain, and f , parametrized by k , is a sufficiently smooth and differentiable function of Z . For example, in the special case when $f(Z; k) \equiv kZ$, k is the angle of twist per unit length of the cylinder. It is noted that this deformation is, in general, inhomogeneous owing to the presence of f . As is evident, this deformation maps a reference cylinder onto a deformed cylinder.

This section is organized as follows. First we present the local (strong) form of the equilibrium equations in cylindrical coordinates. Next we present the variational (weak) form of equilibrium based on energy minimization. Our formulations are consistently Lagrangian. We assume that there are no body forces under consideration and seek to achieve the above deformation by the application of surface tractions alone. It is useful in this context to refer to Ericksen's Theorem, a proof of which can be found in Ogden (1984). The theorem states that homogeneous deformations are the only deformations (of an unconstrained *isotropic* elastic solid) which can be achieved by the application of surface tractions alone independent of the form of the strain energy density function. In the present work, however, we do *not* assume the material to be isotropic and, therefore, Ericksen's theorem does not apply here. Finally, we investigate the correspondence between the two formulations. Establishing this correspondence is not trivial because of the fact that the deformations have been *prescribed* and not obtained as solutions to the classical field equations with boundary conditions. This analysis also enables us to establish conditions on f for equivalence of the two formulations.

3.1. Local form of the static equilibrium equations

It is convenient to perform the present analysis by employing two sets of cylindrical basis vectors. We introduce $\{\mathbf{e}_R, \mathbf{e}_\Theta, \mathbf{e}_Z\}$ as a referential set of basis vectors and $\{\mathbf{e}_r, \mathbf{e}_\theta, \mathbf{e}_z\}$ as a deformed set of basis vectors. These sets of basis vectors are related by a simple orthogonal transformation given as follows (see Fig. 4):

$$\begin{aligned}
 \mathbf{e}_r &= \mathbf{e}_R \cos(f) + \mathbf{e}_\theta \sin(f) \\
 \mathbf{e}_\theta &= -\mathbf{e}_R \sin(f) + \mathbf{e}_\theta \cos(f) \\
 \mathbf{e}_z &= \mathbf{e}_z
 \end{aligned}
 \tag{9}$$

In terms of these basis vectors, the deformation gradient \mathbf{F} can be evaluated to be:

$$\mathbf{F} = \gamma(\mathbf{e}_r \otimes \mathbf{e}_R + \mathbf{e}_\theta \otimes \mathbf{e}_\theta) + \gamma R f' \mathbf{e}_\theta \otimes \mathbf{e}_z + (1 + \epsilon) \mathbf{e}_z \otimes \mathbf{e}_z
 \tag{10}$$

where f' denotes the derivative of f with respect to Z . The corresponding expression for the Lagrangian strain tensor is

$$\mathbf{E} = \frac{1}{2}(\gamma^2 - 1)(\mathbf{e}_R \otimes \mathbf{e}_R + \mathbf{e}_\theta \otimes \mathbf{e}_\theta) + \frac{1}{2}\gamma^2 R f'(\mathbf{e}_\theta \otimes \mathbf{e}_z + \mathbf{e}_z \otimes \mathbf{e}_\theta) + \frac{1}{2}(\gamma^2 R^2 f'^2 + 2\epsilon + \epsilon^2)\mathbf{e}_z \otimes \mathbf{e}_z
 \tag{11}$$

The PKII stress tensor \mathbf{T} is obtained as the derivative of the strain energy density function \hat{W} with respect to the Lagrangian strain \mathbf{E} as follows:

$$\mathbf{T} = \frac{d\hat{W}}{d\mathbf{E}} = \left. \frac{\partial W}{\partial \mathbf{E}} \right|_{\boldsymbol{\eta}} + \left. \frac{\partial W}{\partial \boldsymbol{\eta}} \right|_{\mathbf{E}} \cdot \frac{d\boldsymbol{\eta}}{d\mathbf{E}} = \left. \frac{\partial W}{\partial \mathbf{E}} \right|_{\boldsymbol{\eta}}
 \tag{12}$$

since the relaxed shift vector $\boldsymbol{\eta}$ is chosen such that (refer to earlier discussion on the shift vector):

$$\left. \frac{\partial W}{\partial \boldsymbol{\eta}} \right|_{\mathbf{E}} = \mathbf{0}
 \tag{13}$$

The PKI stress tensor \mathbf{S} is obtained as

$$\mathbf{S} = \mathbf{F} \cdot \mathbf{T}
 \tag{14}$$

Next, we present the referential version of the equilibrium equations without body forces in cylindrical coordinates. First, we assume that the lateral surface of the cylinder is traction-free, i.e.

$$\mathbf{S} \cdot \mathbf{e}_R = \mathbf{0}
 \tag{15}$$

on the outer and inner lateral surfaces. However, since the SWNT has a vanishing wall thickness, we assume (15) to be true through the ‘thickness’ as well. The equilibrium equations in conjunction with (15), along $\{\mathbf{e}_R, \mathbf{e}_\theta, \mathbf{e}_z\}$, respectively, are given as (see, for example [Fung and Tong, 2001](#)):

$$\begin{aligned}
 \frac{1}{R} \frac{\partial S_{R\theta}}{\partial \theta} - \frac{1}{R} S_{\theta\theta} + \frac{\partial S_{Rz}}{\partial Z} &= 0 \\
 \frac{1}{R} S_{R\theta} + \frac{1}{R} \frac{\partial S_{\theta\theta}}{\partial \theta} + \frac{\partial S_{\theta z}}{\partial Z} &= 0 \\
 \frac{1}{R} \frac{\partial S_{z\theta}}{\partial \theta} + \frac{\partial S_{zz}}{\partial Z} &= 0
 \end{aligned}
 \tag{16}$$

Using (9) and (10) in (14), and projecting equations (16) along \mathbf{e}_r gives

$$T_{\theta\theta} + 2Rf'T_{\theta z} + f'^2 R^2 T_{zz} = 0
 \tag{17}$$

Similarly, projecting Eq. (16) along \mathbf{e}_θ gives

$$\frac{\partial T_{\theta\theta}}{\partial \theta} + f'R \frac{\partial T_{\theta z}}{\partial \theta} + R \frac{\partial T_{\theta z}}{\partial Z} + f''R^2 T_{zz} + f'R^2 \frac{\partial T_{zz}}{\partial Z} = 0
 \tag{18}$$

Finally, projecting Eq. (16) along \mathbf{e}_z gives

$$\frac{\partial T_{\theta z}}{\partial \theta} + R \frac{\partial T_{zz}}{\partial Z} = 0
 \tag{19}$$

In addition, the stress measures, in this problem, can be assumed to be independent of the polar coordinate θ . Thus, Eqs. (18) and (19) can be further reduced to

$$\frac{\partial}{\partial Z} [T_{\theta Z} + f'RT_{ZZ}] = 0 \quad (20)$$

$$\frac{\partial T_{ZZ}}{\partial Z} = 0 \quad (21)$$

respectively. Eqs. (20) and (21), along with (17), form the final set of static equilibrium equations in local form for this problem.

3.2. Weak form of the static equilibrium equations: Principle of minimum (stationary) potential energy

The total potential energy of any given deformation map Ψ can be written as

$$\Pi(\Psi) = \Pi_{\text{int}} - \Pi_{\text{ext}} + \Pi_{\text{nb}} \quad (22)$$

where Π_{int} is the internal (strain) energy of the system, given as

$$\Pi_{\text{int}} = \int_{\Omega_0} \hat{W}(\mathbf{E}(\Psi)) \, d\Omega_0 \quad (23)$$

where Ω_0 is the referential/undeformed domain, Π_{ext} contains the body forces and Π_{nb} contains the non-bonded interactions. As mentioned earlier, we do not consider the presence of body forces in the present work. Non-bonded interactions (Arroyo and Belytschko, 2002) which account for forces acting between non-bonded pairs of atoms are also excluded in the present work. According to the principle of stationary energy, the equilibrium configurations of the system, Φ , are stationary points of the potential energy functional. Therefore, we have

$$\delta \Pi(\Phi) \equiv \left. \frac{\partial}{\partial \beta} \Pi(\Phi + \beta \mathcal{Y}) \right|_{\beta=0} = 0 \quad (24)$$

for all admissible variations \mathcal{Y} that satisfy the specified displacement boundary conditions. In connection with the deformation map prescribed in Box 2 and Eq. (11), it is useful, at this stage, to consider \hat{W} as a function of γ , k and ϵ , i.e.

$$\hat{W}(\mathbf{E}) \equiv \tilde{W}(\gamma, k, \epsilon) \quad (25)$$

In the following, we investigate the possibility of satisfying the local equilibrium equations (i.e. Eqs. (20), (21) and (17)) by simply minimizing \tilde{W} with respect to its arguments.

Here, we make the following distinction. If ϵ is imposed and γ and k are determined by minimization, the problem is called an imposed extension problem. On the other hand, if k is prescribed and γ and ϵ are obtained through minimization, the problem is called an imposed twist problem.

3.2.1. Imposed extension problem

In this problem, as mentioned earlier, ϵ is imposed and γ and k are obtained through minimization of \tilde{W} . Accordingly, we require $\frac{\partial \tilde{W}}{\partial \gamma} = 0$. Using this condition, along with Eq. (11) and (12) gives

$$T_{\theta\theta} + 2Rf'T_{\theta Z} + f'^2R^2T_{ZZ} = 0 \quad (26)$$

which is precisely Eq. (17) obtained from the local form of static equilibrium. In addition, we also require $\frac{\partial \tilde{W}}{\partial k} = 0$ which leads to

$$\frac{\partial f'}{\partial k} [T_{\theta Z} + f'RT_{ZZ}] = 0 \quad (27)$$

Assuming $\frac{\partial f'}{\partial k} \neq 0$, we have

$$T_{\theta Z} + f'RT_{ZZ} = 0 \quad (28)$$

which satisfies (20). With regard to satisfying (21), we first note the following relation between the PKII stress and the Cauchy stress:

$$\mathbf{T} = J\mathbf{F}^{-1} \cdot \boldsymbol{\sigma} \cdot \mathbf{F}^{-T} \quad (29)$$

(where $J = \det(\mathbf{F})$) from which we can obtain

$$T_{ZZ} = \frac{\gamma^2}{(1 + \epsilon)} \sigma_{zz} \quad (30)$$

Since σ_{zz} is constant under imposed extension, Eq. (30) implies that (21) is also satisfied. Hence, the imposed extension minimization problem satisfies the required equilibrium equations (without body forces) for arbitrary $f(Z; k)$ satisfying $\frac{\partial f'}{\partial k} \neq 0$.

3.2.2. Imposed twist problem

In this problem, k is imposed and γ and ϵ are obtained through minimization of \tilde{W} . As in Section 3.2.1, we first have $\frac{\partial \tilde{W}}{\partial \gamma} = 0$ which gives Eq. (26) and hence satisfies Eq. (17). In addition, we also require $\frac{\partial \tilde{W}}{\partial \epsilon} = 0$ leading to

$$(1 + \epsilon)T_{ZZ} = 0 \Rightarrow T_{ZZ} = 0 \quad (31)$$

which satisfies (21). Eq. (31), along with (30), also implies

$$\sigma_{zz} = 0 \quad (32)$$

Using (31) in (20), we require:

$$T_{\theta Z} = \text{constant} \quad (33)$$

in order to satisfy the full set of equilibrium equations. Using (29), combined with the result from (32), we can write

$$T_{\theta Z} = \gamma \sigma_{\theta z} \quad (34)$$

Now, we look at small strain theory to generate a *necessary* condition to satisfy (33). From St. Venant's theory of torsion (see, for example Fung and Tong, 2001) and from using Box 2, we can write

$$\sigma_{\theta z} = G\gamma R f' \quad (35)$$

where G is the shear modulus of the material in small strain theory. Finally, from using (35) and (34) in (33), we obtain

$$f' = \text{constant} \quad (36)$$

as the necessary condition to satisfy static equilibrium (without body forces) in the imposed twist problem.

In summary, it is noted that the imposed extension problem satisfies equilibrium for arbitrary f (such that $\frac{\partial f'}{\partial k} \neq 0$), while the imposed twist problem requires the condition $f' = \text{constant}$.

4. Bond vector deformations

In this section, we obtain analytic expressions for the deformed bond vectors between any two atoms denoted by i and j using the CB rule and its modifications. The deformed bond vectors obtained using the direct deformation map serve as a basis for evaluating the accuracy of these deformation rules. Subscripts i and j in the following are used to denote the corresponding coordinates of atoms i and j , respectively.

4.1. Modified Cauchy–Born rule

In the following discussion, the Euclidean bond vectors before and after deformation are denoted by \mathbf{A} and \mathbf{a} , respectively. The projected geodesic vector lying on a tangent plane to the undeformed SWNT is denoted by $\tilde{\mathbf{A}}$, and the deformed geodesic vector (lying on a tangent plane to the deformed SWNT) obtained from directly using the deformation map (Box 2) is denoted by $\tilde{\mathbf{a}}$, while the deformed geodesic vector obtained from the modified CB rule (Arroyo and Belytschko, 2002) is denoted by $\hat{\mathbf{a}}$. As discussed in Section 1, the modified CB rule effectively replaces \mathbf{F} in Eq. (1) by a composition of three operations – first ‘unwrap’ the geodesic connecting the atoms onto the tangent plane at \mathbf{X} (this operation is denoted here by \mathcal{M}), then apply \mathbf{F} to this

geodesic vector to obtain the deformed geodesic vector lying on the deformed tangent plane, and finally ‘wrap’ the deformed geodesic vector back onto the deformed surface (this operation is denoted by \mathcal{M}^{-1}) to obtain the Euclidean bond lengths.

This is graphically shown in Fig. 5, and may be conveniently expressed as follows:

$$\mathbf{a} = \mathcal{M}^{-1}\mathbf{F}(\mathbf{X})\mathcal{M}\mathbf{A} \tag{37}$$

First, the undeformed geodesic vector directed from atom i to atom j , when ‘unwrapped’ onto the undeformed tangent plane at a referential material point is given (in cylindrical coordinates) by

$$\tilde{\mathbf{A}} = \mathcal{M}\mathbf{A} = R(\theta_j - \theta_i)\mathbf{e}_\theta + (Z_j - Z_i)\mathbf{e}_z \tag{38}$$

Next, the deformed geodesic vector obtained by using the direct map given in Box 2 (and also essentially the infinite Taylor series denoted in (3)) can be written as

$$\tilde{\mathbf{a}} = \mathcal{F}(\tilde{\mathbf{A}}) = \gamma R(\theta_j - \theta_i)\mathbf{e}_\theta + (z_j - z_i)\mathbf{e}_z = \gamma R[(\theta_j - \theta_i) + \{f(Z_j) - f(Z_i)\}]\mathbf{e}_\theta + (1 + \epsilon)(Z_j - Z_i)\mathbf{e}_z \tag{39}$$

It is noted that use of the direct map as given by Eq. (3) leads to a higher gradient theory where $W \equiv \hat{W}(\mathbf{F}, \nabla\mathbf{F}, \nabla\nabla\mathbf{F}, \dots)$. Though the definition of stress measures (and hence use of the local formulation) is not as straightforward as in the case when $W \equiv \hat{W}(\mathbf{F})$, the weak formulation (Section 3.2) can still be used directly to perform deformation simulations. Also, comments related to material frame indifference and symmetry made in Section 2.3 apply to the use of the direct map as well.

Now, the deformed geodesic vector is obtained by using the modified CB rule (using Eqs. (38) and (10) in (37)). However, since \mathbf{F} , in general, varies with space in the present analysis, it is evaluated at an intermediate point \mathbf{X}_α lying on the undeformed geodesic vector directed from atom i to atom j , and is given by:

$$\hat{\mathbf{a}} = \mathbf{F}(\mathbf{X}_\alpha) \cdot \tilde{\mathbf{A}} = \gamma R[(\theta_j - \theta_i) + (Z_j - Z_i)f'(Z_\alpha)]\mathbf{e}_\theta + (1 + \epsilon)(Z_j - Z_i)\mathbf{e}_z \tag{40}$$

where Z_α is the undeformed axial coordinate of this intermediate point. Comparing Eqs. (40) and (39), we obtain the location of the point, \mathbf{X}_α , at which the modified CB rule (37) gives the exact solution as obtained from (3). This is obtained as the solution of:

$$f'(Z_\alpha) = \frac{f(Z_j) - f(Z_i)}{Z_j - Z_i} \tag{41}$$

It is noted that since f is assumed to be a differentiable function between Z_i and Z_j , the mean value theorem states that (41) can always be solved to obtain Z_α . It is useful, at this point, to refer back to Section 1 (Eq. (4)) in which a discussion on applying the CB rule for general inhomogeneous deformations is provided in the context of bulk crystals. As a simple illustration of the application of (41), we note that when $f(Z; k) \equiv kZ$, (41) is

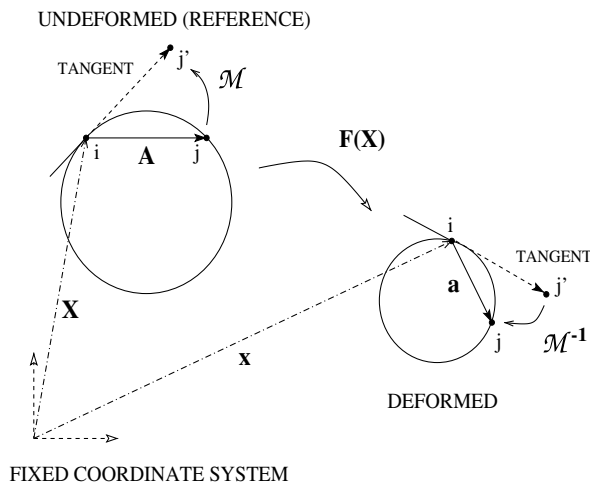


Fig. 5. The modified CB rule for SWNTs modeled as curved manifolds (Arroyo and Belytschko, 2002).

identically satisfied for all choices of \mathbf{X}_α and hence the modified CB rule yields the exact deformed bond vectors (and bond lengths) *independent* of the point at which \mathbf{F} (in (1)) is evaluated. However, if $f(\mathbf{Z}; k) \equiv kZ^2$, Eq. (41) gives the best location to apply the CB rule to be $Z_\alpha = \frac{1}{2}(Z_i + Z_j)$, which corresponds to the mid-point of the ‘unwrapped’ undeformed bond vector. For all other choices of Z_α , the result from the CB rule is clearly only approximate as pointed out in Section 1.

The actual length of the deformed bond vector, i.e. the Euclidean distance between atoms i and j in the deformed configuration (Fig. 5), is obtained by ‘wrapping’ the deformed geodesic (40) back onto the deformed cylinder, and is given by

$$a(i, j) = |\mathbf{a}| = |\mathcal{M}^{-1}\hat{\mathbf{a}}| = \sqrt{\left[4\gamma^2 R^2 \sin^2 \left\{ \frac{1}{2}((\Theta_j - \Theta_i) + (Z_j - Z_i)f'(Z_\alpha)) \right\} + (1 + \epsilon)^2 (Z_j - Z_i)^2 \right]} \quad (42)$$

As mentioned before, for a choice of the ‘unwrap’ point (\mathbf{X}_α) given by Eq. (41), this expression coincides with the exact expression obtained from using the direct deformation map. For *all* other choices of α , this expression is, in general, only approximate. In principle, such an approximation can be improved by adding higher order terms of the Taylor series denoted in (3).

Eq. (42) is used to perform deformation simulations on SWNTs in Section 5. In the following sub-section, we present some general observations on the nature of the deformation gradient \mathbf{F} pertaining to the CB rule, which generalize some of the conclusions drawn in the present section.

4.2. Observations on the deformation gradient related to the Cauchy–Born rule

We consider a setting similar to the one in Section 3.1, and adopt an indicial notation implying summation on all repeated indices. We employ a set of basis vectors $\{\mathbf{e}_I\}$ to describe the undeformed configuration, and a set of basis vectors $\{\mathbf{e}_i\}$ to describe the deformed configuration such that these vectors are related by an orthogonal transformation \mathbf{Q} similar to Eq. (9):

$$\mathbf{e}_i = Q_{iI} \mathbf{e}_I \quad (43)$$

For convenience, we also express the undeformed basis vectors in terms of a fixed Cartesian basis $\{\mathbf{e}_\alpha\}$:

$$\mathbf{e}_I = R_{I\alpha} \mathbf{e}_\alpha \quad (44)$$

and note that $Q_{iI}Q_{jI} = \delta_{ij}$, $R_{I\alpha}R_{J\alpha} = \delta_{IJ}$. It is also to be noted that the basis vectors $\{\mathbf{e}_I\}$, $\{\mathbf{e}_i\}$ and the orthogonal transformations \mathbf{Q} and \mathbf{R} vary in space in general (as also seen from (9) for the cylindrical basis vectors). In terms of these basis vectors, the deformation gradient \mathbf{F} and the undeformed geodesic vector can be expressed (in forms generalizing Eqs. (10) and (38), respectively) as

$$\mathbf{F} = F_{iJ} \mathbf{e}_i \otimes \mathbf{e}_J \quad (45)$$

$$\tilde{\mathbf{A}} = \tilde{A}_I \mathbf{e}_I \quad (46)$$

We note here that the components \tilde{A}_I are constants (cf. with Eq. (38)), while the components F_{iJ} may either be constants or vary in space depending on the specific deformation. In the present deformation considered (Box 2), this depends on the choice of $f(\mathbf{Z}; k)$. From Eq. (10), it is evident that F_{iJ} would be constant in the present case if $f(\mathbf{Z}; k)$ is constant (pure extension problem) or linear (kZ), while it would vary with space otherwise. Using the modified CB rule, one can express the deformed geodesic vector (as a generalized version of Eq. (40)) in terms of the fixed Cartesian basis:

$$\hat{\mathbf{a}} = F_{iJ} \tilde{A}_J Q_{iI} R_{I\alpha} \mathbf{e}_\alpha \quad (47)$$

In Eq. (47), we note that the components of $\hat{\mathbf{a}}$ are inhomogeneous in general owing to the presence of \mathbf{Q} and \mathbf{R} irrespective of whether the components F_{iJ} vary with space. However, the magnitude of $\hat{\mathbf{a}}$ can be found (using the orthogonality of \mathbf{Q} and \mathbf{R}) to be

$$\hat{a} = \sqrt{F_{iJ} F_{iK} \tilde{A}_J \tilde{A}_K} \quad (48)$$

This shows that the deformed geodesic length obtained from the modified CB rule would be independent of the spatial variation in \mathbf{F} if its components F_{iJ} are constants. For the deformations considered in the present work, this also means that the deformed bond lengths would be independent of the spatial variation in \mathbf{F} if its components are constants, which is in agreement with the conclusions drawn from Section 4. Using a similar approach, one can observe that similar conclusions hold even if \mathbf{F} is expressed in a fully referential basis ($\mathbf{F} = F_{IJ}\mathbf{e}_I \otimes \mathbf{e}_J$). In this case, the magnitude of the deformed geodesic vector would be equal to $\sqrt{F_{IJ}F_{IK}\tilde{A}_J\tilde{A}_K}$ and the deformed bond lengths would be independent of the spatial variation in \mathbf{F} if its components F_{IJ} are constants. Finally, as indicated in Chandraseker and Mukherjee (2006), it is straightforward to observe that the standard CB rule (with no modification using the exponential map) gives the exact deformed bond vector if the components of \mathbf{F} are spatially constant with respect to the fixed Cartesian basis (as would occur, for example, in the case of simple tension, or uniform radial expansion/contraction of a circular cylinder) because the gradient-based terms in (3) would simply vanish in such a case.

5. Deformation simulations

In this section, we discuss results for SWNT deformation corresponding to specific choices of $f(\mathbf{Z};k)$ in Box 2.

5.1. $f(\mathbf{Z};k) \equiv k\mathbf{Z}$: Imposed twist and extension problems

Some of the papers that deal with SWNTs under imposed twist and extension (refer to Sections 3.2.2 and 3.2.1) are Jiang et al. (2003), Liu et al. (2004) and Chandraseker and Mukherjee (2006). These studies assume a deformation map as given in Box 2, with $f(\mathbf{Z};k) \equiv k\mathbf{Z}$. As shown in Section 3.2.2 in Eq. (36), this is the only choice for f which can be maintained in equilibrium without body forces for an imposed twist problem. Chandraseker and Mukherjee (2006) performed deformation analysis using the standard CB rule without constraining the atoms to lie on a single surface, and showed that the bond lengths (and the kinematic coupling plots) obtained from the standard CB rule coincided with those obtained from the direct deformation map only for small values of k . This differs from the present approach in which the modified CB rule is used with all the atoms lying on a single surface (the radial component of $\boldsymbol{\eta}$, η_R , is not allowed in the present work – see (7)). In this case, since f' is a constant, Eq. (41) implies that the deformed bond vector (and hence the numerical coupling results – extension obtained under imposed twist) obtained from the modified CB rule is *independent* of the point at which \mathbf{F} is evaluated. Also, Eq. (41) implies that this deformed bond vector is exact (expressions (39) and (40) coincide). This has, however, been shown to *not* be true if the standard CB rule is used (Chandraseker and Mukherjee, 2006), and hence the exponential map modification becomes essential in this case to obtain the exact bond lengths.

Here, we present kinematic coupling results (using the modified CB rule, and $\eta_R = 0$) for imposed twist in Fig. 6(a) and (b), and imposed extension in Fig. 6(c) and (d), for representative chiral (9, 6), zig-zag (10, 0) and armchair (5, 5) SWNTs corresponding to parameter set 1 of the Brenner (1990) interatomic potential. In Fig. 6(a), we observe a small decrease in the radii of the SWNTs for large values of the twist parameter k . In Fig. 6(b), it is observed that the chiral nanotube exhibits an asymmetric coupling between extension and twist, for imposed twist. The armchair and zig-zag nanotubes, however, exhibit a symmetric extension $\epsilon(k)$ about $k = 0$ owing to their nominally axisymmetric atomic structure (see, for example Chandraseker and Mukherjee, 2006). Further, the chiral nanotube exhibits the largest $|\epsilon|$ for large values of $|k|$. In the case of imposed extension, it is noted that, as expected, the radius changes caused by extension (Poisson effect, Fig. 6(c)) are, in general, much larger than those caused by twist (Fig. 6(a)). As expected, the chiral nanotube twists under imposed extension (Fig. 6(d)), while the armchair and zig-zag nanotubes do not (i.e. the induced twist for the armchair and zig-zag nanotubes is zero throughout the range of imposed extension). This is related to the fact that the chiral nanotube has an asymmetric bond structure while the armchair and zig-zag nanotubes are nominally symmetric about the cylinder axis.

Finally, we mention here that a ‘simplified’ version of the Brenner (1990) potential is employed in the present work. (This same simplified version has been used previously by Zhang et al. (2002), Jiang et al. (2003), Liu

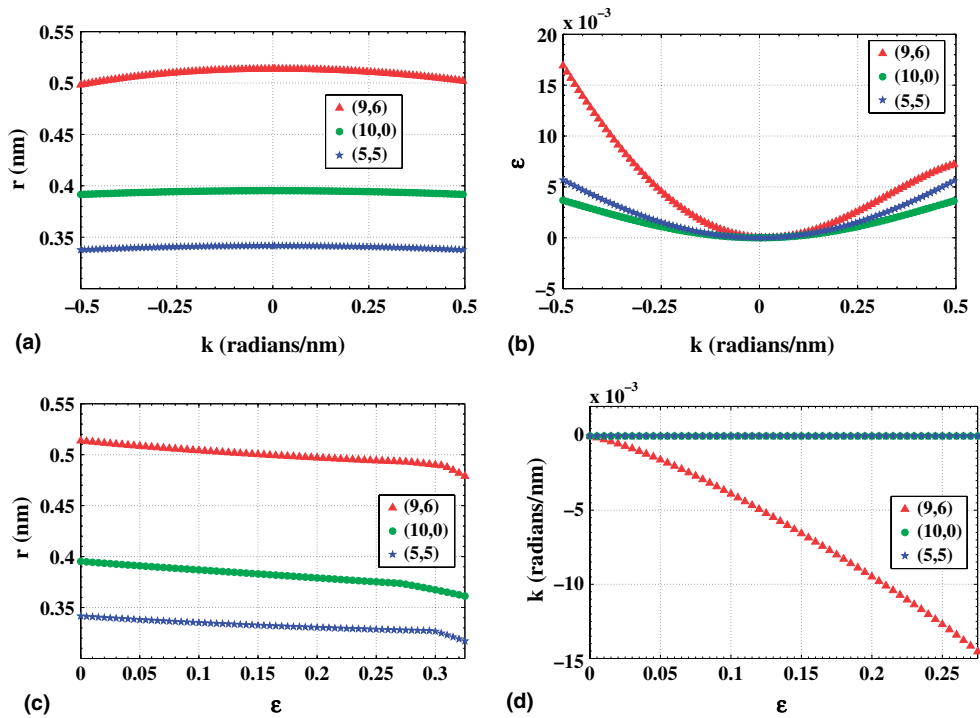


Fig. 6. Kinematic coupling plots for representative chiral (9,6), zig-zag (10,0) and armchair (5,5) SWNTs corresponding to $f(Z;k) \equiv kZ$, using parameter set 1 of the Brenner (1990) potential.

et al. (2004) and Chandraseker and Mukherjee (2006)). In particular, $F(i,j)$ (called F_{ij} in Brenner, 1990) is assumed to be zero in the expression for $\bar{B}(i,j)$ (called \bar{B}_{ij} in Brenner, 1990) in Eq. (10) of Brenner (1990). The primary reason for doing this is to employ an analytically convenient form of the interatomic potential (there is no intrinsic difficulty in using the full Brenner (1990) expressions). The consequences of using this form of the potential are discussed in detail in Chandraseker and Mukherjee (2006). It has been observed that the assumed form is exact for this class of problems for imposed strains of upto about 30% (after which the bond order of some of the carbon atoms changes – bonds may break and new bonds may form). This is in agreement with some earlier results on tensile yield strains of SWNTs using molecular-dynamics calculations at temperatures of about 600 K (Yakobson, 1998; Yakobson et al., 1997). In particular, Yakobson et al. (1997) report a strong temperature dependence on the value of the yield strain (with values as high as 55% at 50 K, decreasing to about 25% at 1200 K) and a weak dependence on the chirality of the SWNTs. The assumed form is, however, exact for the imposed twist problem throughout the plotted range of imposed k ($-0.5 \leq k \leq 0.5$) because no changes are observed in the bond orders of the carbon atoms throughout this range of imposed k .

5.2. $f(Z;k) \equiv kZ^2$: Imposed extension problem

Here, we present numerical results for imposed extension problems with $f(Z;k) \equiv kZ^2$ (this satisfies the conditions obtained in Section 3.2.1). Since this choice of deformation ($f(Z;k) \equiv kZ^2$) is difficult to realize physically, we present plots of the deformed energy/atom (instead of kinematic coupling plots), i.e., the binding energy/atom (E_b) for representative chiral (9,6), zig-zag (10,0) and armchair (5,5) SWNTs using parameter set 1 of the Brenner (1990) interatomic potential. For this choice, Eq. (41) gives the best location to apply the modified CB rule to be $Z_\alpha = \frac{1}{2}(Z_i + Z_j)$ (note that since α lies on the geodesic connecting i and j , one also has $\Theta_\alpha = \frac{1}{2}(\Theta_i + \Theta_j)$), henceforth referred to as the ‘mid point rule’, where the deformed bond vectors obtained from the direct map and the modified CB rule coincide. We also present results from applying the

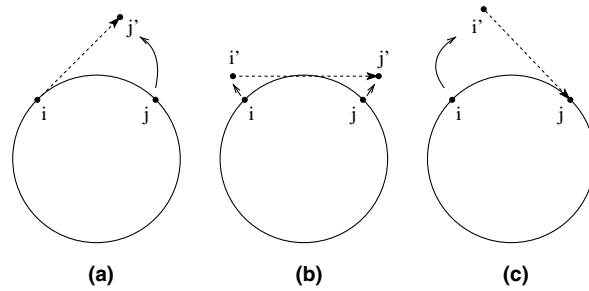


Fig. 7. Various ‘unwrapping’ rules – (a) start point, (b) mid point and (c) end point.

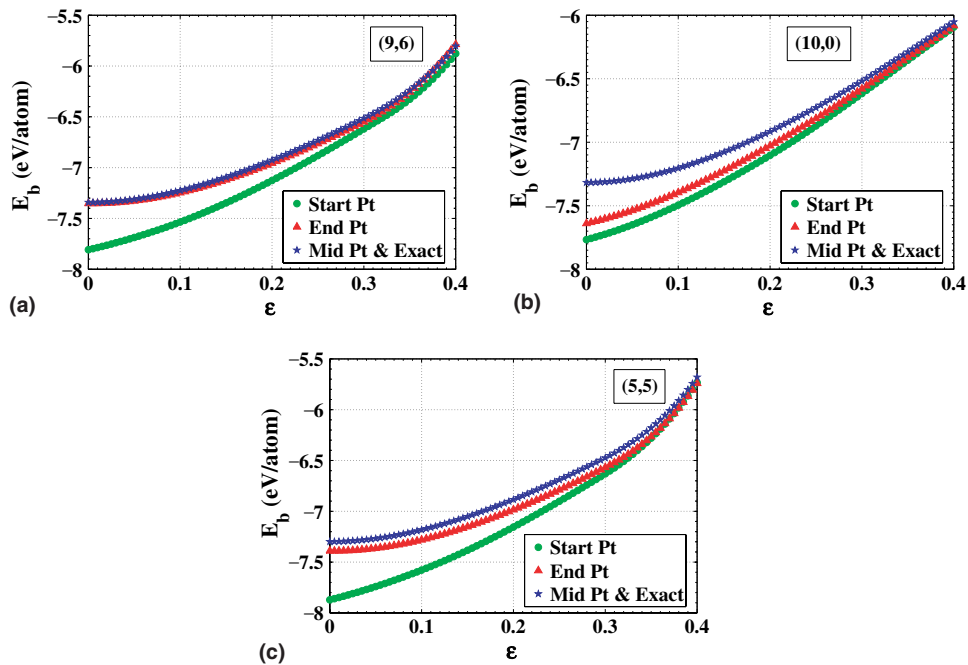


Fig. 8. Comparison of binding energy/atom (E_b) from different rules for representative (a) chiral (9,6), (b) zig-zag (10,0), and (c) armchair (5,5) SWNTs corresponding to $f(Z;k) \equiv kZ^2$, using parameter set 1 of the Brenner (1990) potential. Results from the ‘mid point’ rule coincide exactly with those from the direct map (here called the exact solution).

modified CB rule at the locations of each of the two atoms, i and j . These are denoted as the ‘start point rule’ and the ‘end point rule’, respectively. Fig. 7 illustrates these different ‘unwrapping’ rules.

In Fig. 8, the energy/atom (as a function of imposed ϵ) obtained using the three deformation rules mentioned above, are compared for each type of SWNT. It is observed, as expected, that for all the SWNTs, results from the ‘mid point rule’ coincide exactly with those from the direct deformation map (referred to as the exact solution). The results from the ‘start point’ and ‘end point’ rules, however, do not agree with the exact solution – again, as expected from the discussion in Section 4.

6. Concluding remarks

The following remarks are in order:

- The modified Cauchy–Born (CB) rule has been employed to study deformations that are assumed to be inhomogeneous at the atomic scale. For a specific class of generalized extension–twist deformations on

SWNTs, the present work deals with determining a point (on the undeformed bond) at which to evaluate \mathbf{F} in the modified CB rule (37) so that the deformed bond vectors coincide with the exact expression given by the direct map.

- Numerical results are presented for extension–twist problems with $f(\mathbf{Z};k) \equiv k\mathbf{Z}$ and $f(\mathbf{Z};k) \equiv k\mathbf{Z}^2$ (see Box 2). The ‘mid point rule’ (see Section 5) is analytically shown to give a deformed bond vector coincident with the exact expression determined from the map. Numerical results for imposed extension are presented for this problem using the ‘mid point rule’ as well as the ‘start point’ and ‘end point’ rules (Section 5). It is analytically shown that in the case when $f(\mathbf{Z};k) \equiv k\mathbf{Z}$, the deformed bond lengths obtained from the modified CB rule coincide with the exact solution (Section 4) independent of the point at which \mathbf{F} is evaluated. However, when $f(\mathbf{Z};k) \equiv k\mathbf{Z}^2$, the ‘mid point rule’ alone gives the exact solution while the ‘start point’ and ‘end point’ rules do not.
- For more complicated deformations, the ‘mid point rule’ does not, in general, yield the exact solution. However, in these cases, if a *deformation map is available*, the mean value theorem can easily be utilized to obtain a location at which the CB rule gives the exact solution (see Eq. (41)).
- In the absence of a generalization of the modified CB rule for inhomogeneous deformations *without an explicit deformation map*, the ‘mid point rule’ could still be heuristically recommended based on the fact that the mid point is ‘unbiased’ relative to any other point on a bond, and is proposed here as a good choice for future work. A simple Taylor series calculation shown in [Appendix A](#) lends further support to this idea.

Acknowledgement

This research has been supported by Grant # EEC-0303674 of the National Science Foundation to Cornell University.

Appendix A

Let x_i and x_j denote points on a curve parameterized by s , with curvilinear coordinates s_i and s_j , respectively. Let x_m denote the mid point between x_i and x_j , and s_m denote its curvilinear coordinate. Then, for an arbitrary function $\phi(x)$ (assumed to be sufficiently smooth and differentiable in $[x_i, x_j]$) defined on the curve, and $\xi_1 \in [x_i, x_m]$, $\xi_2 \in [x_m, x_j]$:

$$\phi(x_i) = \phi(x_m) + (s_i - s_m)\phi_{,s}(x_m) + \frac{1}{2!}(s_i - s_m)^2\phi_{,ss}(\xi_1) \quad (49)$$

$$\phi(x_j) = \phi(x_m) + (s_j - s_m)\phi_{,s}(x_m) + \frac{1}{2!}(s_j - s_m)^2\phi_{,ss}(\xi_2) \quad (50)$$

where, s denotes derivative with respect to s . Now, if ϕ is assumed to be quadratic, $\phi_{,ss}(\xi_1) = \phi_{,ss}(\xi_2)$. Using this, along with the fact that x_m is the mid point, and subtracting Eq. (49) from Eq. (50) gives

$$\phi(x_j) - \phi(x_i) = \phi_{,s}(x_m)(s_j - s_i) \quad (51)$$

which amounts to Eq. (41) for a quadratic f evaluated using the ‘mid point rule’. Further, if ϕ is of any higher degree (than quadratic), Eq. (41) can be readily employed to obtain a location $x_{\text{exact}} \in [x_i, x_j]$ at which

$$\phi(x_j) - \phi(x_i) = \phi_{,s}(x_{\text{exact}})(s_j - s_i) \quad (52)$$

References

- Arroyo, M., Belytschko, T., 2002. An atomistic-based finite deformation membrane for single layer crystalline films. *J. Mech. Phys. Solids* 50, 1941–1977.
- Brenner, D.W., 1990. Empirical potential for hydrocarbons for use in simulating the chemical vapor deposition of diamond films. *Phys. Rev. B* 42, 9458–9471.
- Chandraseker, K., Mukherjee, S., 2006. Coupling of extension and twist in single-walled carbon nanotubes. *ASME J. Appl. Mech.* 73 (2), 315–326.

- Cousins, C., 1978. Inner elasticity. *J. Phys. C* 11, 4867–4879.
- Dresselhaus, M.S., Dresselhaus, G., Jorio, A., 2004. Unusual properties and structure of carbon nanotubes. *Annu. Rev. Mater. Res.* 34, 247–278.
- Ericksen, J.L., 1984. The Cauchy and Born Hypotheses for crystals. In: Gurtin, M.E. (Ed.), *Phase Transformations and Material Instabilities in Solids*. Academic Press, New York, pp. 61–77.
- Fung, Y.C., Tong, P., 2001. *Classical and Computational Solid Mechanics*. World Scientific, Singapore.
- Gradshteyn, I.S., Ryzhik, I.M., 2000. *Tables of Integrals, Series, and Products*, sixth ed. Academic Press, San Diego, CA, pp. 1097–1098.
- Jiang, H., Zhang, P., Liu, B., Huang, Y., Geubelle, P.H., Gao, H., Hwang, K.C., 2003. The effect of nanotube radius on the constitutive model for carbon nanotubes. *J. Comput. Mater. Sci.* 28, 429–442.
- Liu, B., Jiang, H., Johnson, H.T., Huang, Y., 2004. The influence of mechanical deformation on the electrical properties of single wall carbon nanotubes. *J. Mech. Phys. Solids* 52, 1–26.
- Marsden, J.E., Hughes, T.J., 1983. *Mathematical Foundations of Elasticity*. Prentice-Hall, Englewood Cliffs, NJ.
- Ogden, R.W., 1984. *Non-linear Elastic Deformations*. Ellis Horwood Series in Mathematics and its Applications, Chichester, UK.
- Shenoy, V., Miller, R., Tadmor, E., Rodney, D., Phillips, R., Ortiz, M., 1999. An adaptive finite element approach to atomic-scale mechanics – the quasicontinuum method. *J. Mech. Phys. Solids* 47, 611–642.
- Steigmann, D.J., Ogden, R.W., 1999. Elastic surface-substrate interactions. *Proc. R. Soc. Lond. A* 455, 437–474.
- Tadmor, E., Smith, G., Bernstein, N., Kaxiras, E., 1996. Quasicontinuum analysis of defects in solids. *Philos. Mag. A* 73 (6), 1529–1563.
- Tadmor, E.B., Smith, G.S., Bernstein, N., Kaxiras, E., 1999. Mixed finite element and atomistic formulation for complex crystals. *Phys. Rev. B* 59, 235–245.
- Tersoff, J., 1988. New empirical approach for the structure and energy of covalent systems. *Phys. Rev. B* 37, 6991–7000.
- Yakobson, B.I., 1998. Mechanical relaxation and “intramolecular plasticity” in carbon nanotubes. *Appl. Phys. Lett.* 72, 918–920.
- Yakobson, B.I., Campbell, M.P., Brabec, C.J., Bernholc, J., 1997. High strain rate fracture and C-chain unraveling in carbon nanotubes. *J. Comput. Mater. Sci.* 8, 341–348.
- Zhang, P., Huang, Y., Geubelle, P.H., Klein, P.A., Hwang, K.C., 2002. The elastic modulus of single-wall carbon nanotubes: a continuum analysis incorporating interatomic potentials. *Int. J. Solids Struct.* 39, 3893–3906.